THE RHEODYNAMICS AND COMBUSTION OF COAL-WATER MIXTURES

by

A. P. Burdukov, V. P. Popov and V. D. Fedosenko

Original scientific paper
UDC: 662.612/.613:66.088
BIBLID: 0354–9836, 2 (1998), 2, 45–59

Special research methods were developed for studying a flow in a tube and the dynamics of the combustion and gasification of a single drop. For a laser-heated small fuel particle, combustion dynamics and gasification were studied with automatic measurement and data processing for its temperature, and its photo-electric and gas-analytic characteristics. From the combustion of a drop of coal-water mixture, we demonstrated that these methods enable the investigation of thermometric, pyrometric and concentrational dynamics for the combustion of a single fuel drop. This technique gives us the total combustion time, it registers the duration of the combustion phases, the moment and the temperature of the drop's ignition, and it gives us information about the combustion mass rate and the products of gasification. It is possible to control the duration of the combustion process through fuel composition in coal-water mixtures: the ratio of a fast-reactive component to a slow-reactive one.

Introduction

The coal-water mixture (CWM) is a new kind of fuel suitable both for large-scale and small-scale power plants [1]. The practical interest in this kind of fuel is due to its technological and economical aspects: the fuel deposits are usually far away from the consumption sites. CWM has several advantages in comparison with regular micronized coal fuel: these fluidized reactive mixtures can be transported over long distances through pipelines, safety requirements are met, and the burning of this fuel yields a lesser quantity of pollution – oxides of sulfur, nitrogen, *etc*. Expensive heavy oil can be substituted for another fuel.

Nowadays CWM is used in many industrial countries. Russia also is having positive experiences in the production, transportation and the combustion of coal-water mixtures (CWM). Being prepared in "Ugleprovod, Ltd." (Belousovo) the coal-water mixture is supplied through a 298 km-long pipeline to the Heat Power Station N5 in Novosibirsk. The solid fraction (62%) is the coal from the Inskaya mine in Belovo-city (Kuznetsk deposit). The dispersed media is water (37%), and the rest 1% is a plastificator

– sulfate salts of naphthalene-formaldehyde with surfactant properties (the admixture C-3). The solid phase of the CWM has a grain-size in the range of 20–350 μm. The technology specification for the CWM supplied to boilers dictated the level of viscosity at about 800 centipoise.

Regardless of the listed advantages of CWM, its wide usage is restricted by the insufficient knowledge of mechanisms and other factors governing its transportation, ignition conditions, and gasification.

Rheological properties of CWMs

The solid fraction in our experiments with CWM was prepared from different types of coal: anthracite graded as ASS (1–13 μm) from Gorlovka deposit (Novosibirsk) – the slow-reactive but high-calorific component; fast-reactive coal with the *D*-grade from Kuznetsk deposit, and lignite from Kansk-Achinsk and East-Siberia deposits. The main physical and chemical characteristics of these coals are summarized in the Table 1. The ASS anthracite and lignite coals were crumbled up in a laboratory mill. The powder from Kuznetsk coal ($R_{x_{90}} = 27\%$, $R_{x_{200}} = 4\%$) was sampled from random sites within the hammer mill volume at the Novosibirsk's Heat Station N5. Using a regular procedure [2], we obtained the mixture with the following composition: 0–68 μm – 62%; 68–100 μm – 15%; 100–160 μm – 15%; 160–200 μm – 4%; 200–315 μm – 4%. This composition is very close to that used for pipeline transportation from Belovo to Novosibirsk.

Table 1. Coal characteristics

N	Coal	Ash content basis (dry weight)	Moisture content (as resived basis)	Low margin of the calorific value	Sulfur content	Volatile compone nts yield
1	Lignite	7–10%	35–38%	4244 W	0.6%	46.5%
2	Anthracite	18%	10%	6709 W	0.3%	39%
3	Coal grade D	10%	16.6%	6105 W	0.3	39%
4	Coal grade B3P	22%	23%	4674 W	0.9%	43%
5	Coal grade DD2	19.4%	6%	6453 W	0.4%	45%
6	Coal grade 2B	15%	36%	3965 W	0.5%	43%

The "dry coal" composition was 60%, and the percentage of "enlighten" water in the mixture was 40% (pH=11.5 after ash removal). There was no plastificator in the mixture.

The problem of the mixture's sedimentation stability, hydraulic transportation and its pulverization requires for information of its fluidity properties and time stability. These parameters were investigated in the automatic regime on the rotation viscosimeter Rheotest-2 [3]. Experiments (Fig. 1) were performed for the shear velocity of D = 5.4–48.6 s^{-1} (t = 20 °C). The prepared CWM (used as the reserved fuel) has a reasonable operational viscosity η=1.5 Pa·s at D=48.6 s^{-1}. Figure 2 confirms that viscosity of CWM is stable for the studied time interval.

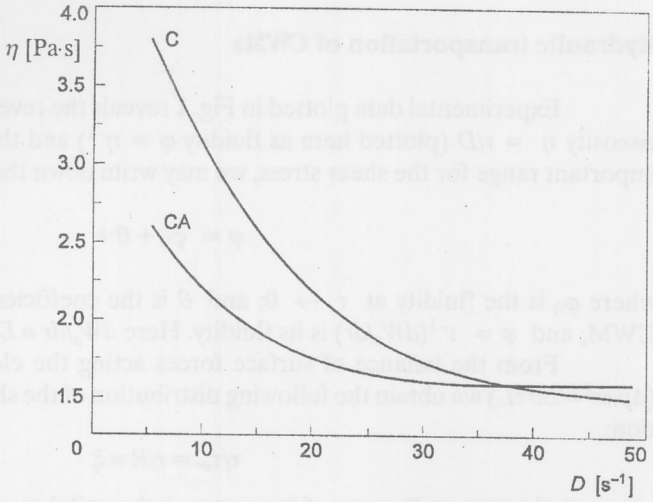

Figure 1. Rheological properties of CWM: *C* – CWM prepared from the *D*-grade coal (Kuznetsk deposit); CA – CWM prepared from the mixture of high-reactive D-grade coal (Kuznetsk) and 5% of low-reactive ASS-grade coal

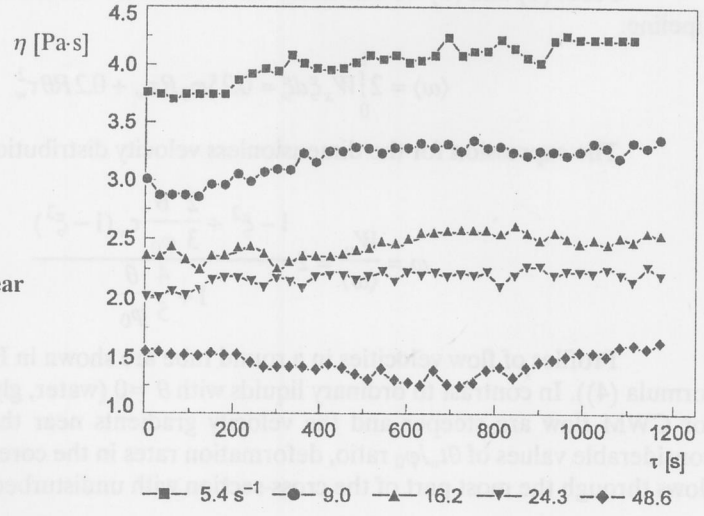

Figure 2. CWM's viscosity *vs.* time and shear velocity (tixotropic properties)

Our experiments on CWM rheology were performed without a plastificator. However, our test on the effect of the regular C-3 admixture on the sedimentation resistance demonstrated that this 1% admixture (from the solid amount) to the SWM makes the sedimentation of the solids by 3 times longer – under the conditions of a natural convection. Under the conditions of uniform forced convection, the effect of the admixture on sedimentation time was insignificant. However, the effect of small media-affecting admixtures on CWMs transported for a long distance, requires for special study. This is due to hydrodynamic maldistributions which may occur both along the pipe and across it.

Hydraulic transportation of CWMs

Experimental data plotted in Fig. 1 reveals the reverse relationship between the viscosity $\eta = \tau/D$ (plotted here as fluidity $\varphi = \eta^{-1}$) and the shear stress. For the most important range for the shear stress, we may write down the following ratio:

$$\varphi = \varphi_0 + \theta \cdot \tau \tag{1}$$

where φ_0 is the fluidity at $\tau \to 0$; and θ is the coefficient of structural instability of CWM; and $\varphi = \tau^{-1}(dW_x/dr)$ is its fluidity. Here $dW_x/dr \equiv D$.

From the balance of surface forces acting the elementary pipeline's cylinder ($\Delta p \pi r^2 = 2\pi r \tau L$) we obtain the following distribution of the shear stress over the cross-section:

$$\tau/\tau_w = r/R \equiv \xi \tag{2}$$

where r is the current diameter of the pipe; τ_w is the wall shear stress – it equals $\tau_w = \Delta pR/2L$, (Δp – pressure drop, R – tube radius, L – is the tube over which this pressure drop $\Delta p = p_1 - p_2$ occurs).

From (1) and (2) we can make the formula for the mean velocity of CWM in a pipeline:

$$\langle \omega \rangle = 2\int_0^1 W_x \xi d\xi = 0.25\varphi_0 R\tau_w + 0.2R\theta\tau_w^2 \tag{3}$$

The expression for the dimensionless velocity distribution is as follows:

$$\omega = \frac{W_x}{\langle \omega \rangle} = 2\frac{1 - \xi^2 + \frac{2}{3}\frac{\theta}{\varphi_0}\tau_w(1 - \xi^3)}{1 + \frac{4}{5}\frac{\theta}{\varphi_0}} \tag{4}$$

Profiles of flow velocities in a round tube are shown in Fig. 3 (calculated by the formula (4)). In contrast to ordinary liquids with $\theta = 0$ (water, glycerin, oil), the profiles for CWM flow are steeper and the velocity gradients near the wall are higher. For considerable values of $\theta t_w/\varphi_0$ ratio, deformation rates in the core flow are low, so CWM flows through the most part of the cross-section with undisturbed structure.

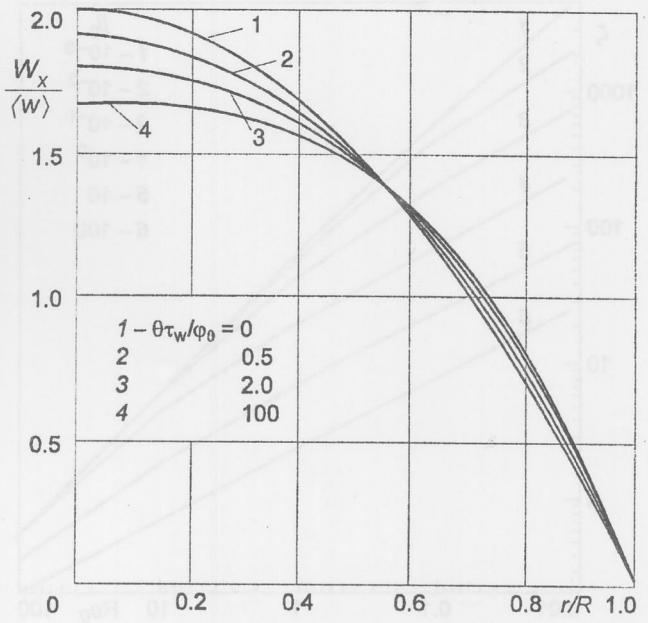

Figure 3. Velocity profiles for CWMs pumped through a round tube depending on the structural-mechanical factor $\theta\tau_w/\varphi_0$

Structural changes in the medium (out of the flow core) causes a nonlinear dependency between the pressure drop and flow rate for a CWM [see formula (3)]. Thus, the change in the pressure drop along the pipeline makes ambiguous effect on the flow rate, as well as on its heat and mass transfer, for instance between the tube and soil, and in the tube-shell heat exchangers for CWM heaters, *etc.*

Regarding formula (3), the expression for the drag coefficient of CWM flow in a round tube takes the form:

$$\zeta = \frac{8\tau_w}{\rho\langle\omega\rangle^2} = \frac{5}{\beta_0}\left[\left(1+\frac{128}{5}\frac{\beta_0}{\mathrm{Re}_0}\right)^{0.5} - 1\right] \qquad (5)$$

where $\beta_0 = \dfrac{\theta}{\varphi_0}\rho\langle\omega\rangle^2$; $\mathrm{Re}_0 = \varphi_0\rho\langle\omega\rangle d$.

For a certain coal-water mixture, characterized by the structural parameter β_0 and for a given pipeline capacity, one can calculate the required pressure drop.

Calculation data from formula (5) are presented in Fig. 4. It is obvious that CWM media structuring reduces the flow resistance. This is caused by a higher fluidity of CWM near the wall. Fluidity increases with dissipation of the CWM structure and successive orientation of solid asymmetrical particles along the streamlines – due to the action of shear velocity gradient.

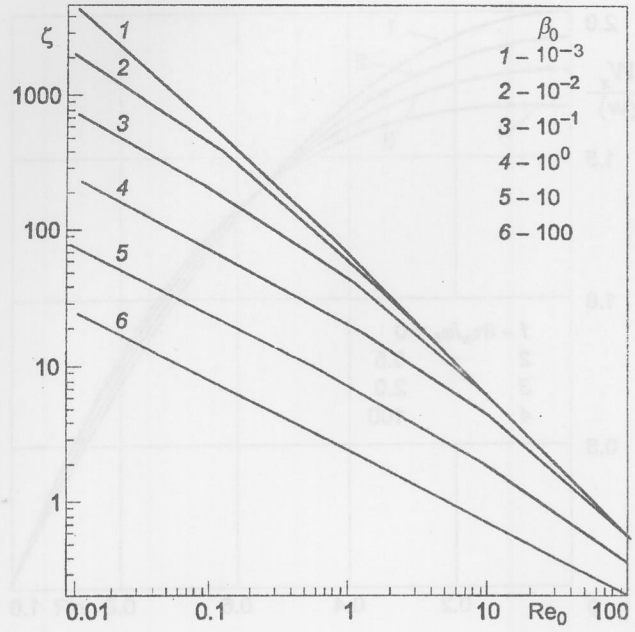

Figure 4. CWM flow in a round tube. The resistance coefficient as a function of the Reynolds number $Re_0 = \varphi_0\rho\langle\omega\rangle d$ and parameter $\beta_0 = (\theta/\varphi_0)\rho\langle\omega\rangle^2$

Technique for investigation of CWM combustion

The difference in the sizes of furnaces and dispersed fuel drops is enormous. Therefore the main information concerning CWM combustion and gasification (*e.g.*, ignition temperature, time of water evaporation from a drop, complete gasification time, diameter of pulverized drops can be obtained by studying single drops [4].

To ignite a small amount of fuel, several methods of heating are available (ohmic heating, plasma, spark discharge, *etc.*). None of them allows us to trace down the real dynamic of combustion for a wide temperature range (especially, at the beginning). The plasma and spark method make inconveniences by direct contact between the drop and ambient medium. The ohmic heating is limited with its temperature (below 1200 °C). It is also hard to study the initial stage of combustion because the time of the drop deliver to the desired place in the furnace is about the time of initial processes: heating-up, water evaporation and evaporation of volatile components. In our experiments the heating of an immovable CWM drop begins from the opening of the laser's shutter. Unlike the ohmic technique, the laser heating method allows us to perform experiments at higher temperatures, to study the dynamics of combustion [5] and gasification of small fuel drops, providing automatic measuring of the temperature, photoelectric characteristics and to perform gas analysis.

The experimental setup (Fig. 5) includes the CO_2-laser (wavelength – 10.6 μm, N~25 W) with water cooling. The adjusted and partially diaphragmed beam passes

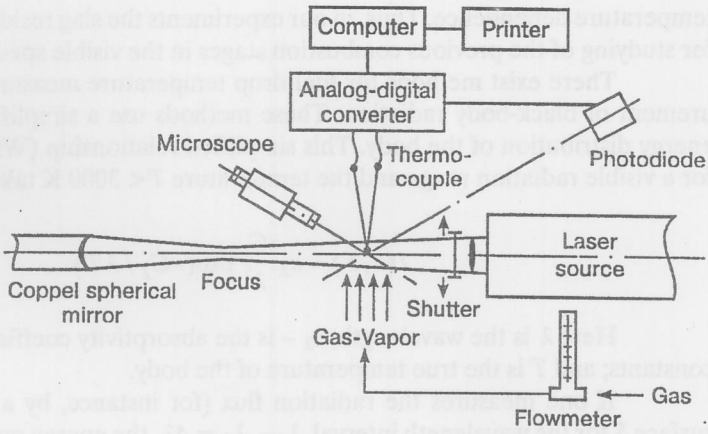

Figure 5. The general scheme of the setup for fuel drop combustion and data processing

through optical lens made from BaF_2. Laser radiation comes to the drop's hemisphere at the thermocouple junction. The power of laser radiation can vary due to a longitudinal shift (transfocal shift) of optical lens, and due to an admissible current drift at the high-voltage laser source. Since the light beam diameter is by order greater than the drop's diameter, the unused portion of radiation is forced to returned using a copper spherical mirror at the opposite side of the hemisphere. Therefore, the amount of light energy at both hemispheres of the drop must be the same. This may be achieved by accurate calculation (of the focus distance) and positioning of the thermocouple's junction. To reduce the heat losses through the thermocouple's wires, the 2-mm section nearby the junction was positioned along the beam axis. The thermocouple (Pt – Pt with 10%Rh) was manufactured from a wire with 100 μm in diameter. The junction diameter did not exceed 120 μm. The heat and cooling time testing revealed that the thermocouple's time constant is less than the time scale of combustion phases – it is about 0.25 s. The thermocouple was fixed at a collet hemispheric hinge to provide easy fitting to the beam. There were two visible-light photodiodes placed at a small angle to the laser beam.

This way we were able to measure both thermometric (contact) and pyrometric (color) temperature [6]. Unlike the first approach, the radiation technique for temperature measurement has less inertia, so the temperature-time pattern of combustion stages (combustion of volatile components and coke residues) and data on the combustion mass rate are more detailed. However, it is better to use thermocouples for measuring of the drop heating stage, when the radiation spectrum is in the infrared region. For this temperature range, there was no combustion yet, so this thin Pt–Pt/Rh thermocouple is reliable for tracking down heat disturbances.

A crucial point in pyrometric analysis is to determine the absorptivity of the emitting medium during combustion. For this method, it can be find out from the algorithmic solution of the reverse problem for the absorptivity parameter (slag after combustion) relative the equilibrium temperature (thermometric technique). In this case we assume that optical properties of the slag and the burning drop are identical; another assumption is that absorptivity of all phases of burning medium has a slight

temperature dependence. Thus, in our experiments the slag residue's absorptivity is used for studying of the previous combustion stages in the visible spectrum.

There exist methods for fuel drop temperature measurement using the measurement of black-body radiation. These methods use a simplified Plank's law for the energy distribution of the body. This simplified relationship (Wien's displacement law) for a visible radiation range and the temperature $T< 3000$ K takes the form:

$$I(\lambda,T)=\varepsilon_\lambda \frac{C_1}{\lambda^5}\exp(-C_2/\lambda T)\ldots \tag{6}$$

Here λ is the wavelength; ε_λ – is the absorptivity coefficient; C_1, C_2 are Plank's constants; and T is the true temperature of the body.

If one measures the radiation flux (for instance, by a photodiode) from the surface S for the wavelength interval $\lambda_1-\lambda_2=\Delta\lambda$, the energy radiation within the space angle ω is described by the formula:

$$I(T)=\int_{\omega}\int_{F}\int_{\lambda} I(\lambda,T)d\lambda dS d\omega\ldots \tag{7}$$

Taking relationships (6) and (7), one can calculate the true temperature of the body T. The main difficulty is that for calculation of the true temperature one have to know the space angle of observation ω, the emitting area and the spectral absorptivity coefficient.

If the experiment is conducted with the two-point registration scheme (two photodiodes) – two wavelengths – the logarithmic form the relationship (6) is as follows:

$$\ln I_{(i)}=\ln\varepsilon_{\lambda i}-5\ln\lambda_i+\ln C_1-C_2/\lambda_i T$$

where $i=1, 2$

or

$$\ln\left(\frac{I_{\lambda_1}}{I_{\lambda_2}}\right)=\ln\frac{\varepsilon_{\lambda_1}}{\varepsilon_{\lambda_2}}-5\ln\frac{\lambda_1}{\lambda_2}+\frac{C_2}{T}\left(\frac{1}{\lambda_2}-\frac{1}{\lambda_1}\right)\ldots$$

Therefore, the color-technique measured temperature is the following:

$$T=\frac{C_2\left(\lambda_2^{-1}-\lambda_1^{-1}\right)}{\ln\left(\frac{I_{\lambda_1}}{I_{\lambda_2}}\right)+5\ln\frac{\lambda_1}{\lambda_2}-\ln\frac{\varepsilon_{\lambda_1}}{\varepsilon_{\lambda_2}}}\ldots \tag{8}$$

We see from formula (8) that for calculating T we need information about two wavelengths for which measuring is carried out, and data about the selectivity of the emitting source. There are two variants. If the photodetectors with narrow-band filters perceive light energy at a specific wavelength, the problem of calculation of T reduces to obtaining of the drop's emissivity for the two wavelengths.

If our photodetectors obtain energy of light at unknown wavelength (wide-band spectrum), then the algorithm of calculation of T must include the wavelength calibration of photodetectors. This testing is executed according to Wien's law (6) with assumption of black-body emission at two specific temperatures.

$$\ln \frac{I_{T_2}}{I_{T_1}} = \frac{C_2}{\lambda}\left(\frac{\Delta T}{T_1 T_2}\right)\ldots \tag{9}$$

It was mentioned above that, according to equation (8), the crucial point of calculation of the true temperature from measured the color temperature– T_c is our prior knowledge about emissivity of the medium at two wavelength λ_1 and λ_2. In our experiments this problem is solved by finding of $\ln \varepsilon_{\lambda_1}/\varepsilon_{\lambda_2}$ from thermometric measurements in the temperature equilibrium range with assumption of ε_{λ_1} and ε_{λ_2} being independent of the temperature. Another assumption is that elementary content of the emitting substance is stable.

These two supplementary methods (thermometric and pyrometric), for studying the dynamics of a small fuel drop combustion with the following computer processing, allow us to study in detail the temporal combustion phases (for a wide range of fast processes), and to determine the mass of fuel, which burns per time unit and per surface unit.

To determine this parameter, we can write down the heat balance of a burning immovable (Re $\rightarrow$ 0) particle in air with a one-side radiation into the ambient medium.

For a small particle we have Bio's criterion Bi $= \alpha_k d/2\lambda < 1$, Fourier's criterion Fo $= (a\tau_* / d^2) \gg 1$. Here a, λ, τ_*, d are the temperature conductivity, heat conductivity, burn-out time, and the particle diameter, correspondingly. That is, we can assume that the temperature gradient across the particle is small (external heat and mass transfer) and the change in the internal energy due to nonstationary effects is negligible.

Our experiments (Fig. 6) demonstrated that a carbon particle burns in air mainly into CO_2. Since molecular weights of air and CO_2 are close, we may write down the Lewis criterion as Le $= D/a \sim 1$. Therefore, the similarity between the temperature and

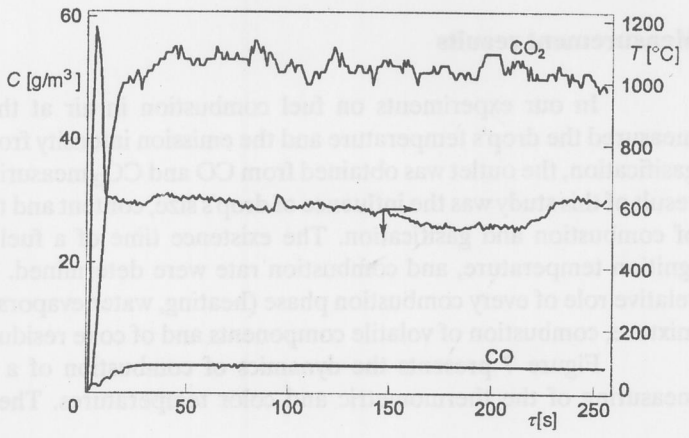

Figure 6. Dynamics of CO_2 and CO concentration during CWM drop (d = 1.5 mm) combustion. The mixture of D–grade coal from Kuznetsk deposit and 5% of ASS–grade coal

concentration fields takes place in the outer combustion zone. Therefore, these conditions Re→0, Fo ≫1, Bi < 1, Le~1, with all the mentioned assumptions concerning emissivity coefficients of the burning particle and slag, give us the opportunity to write down the heat balance equation:

$$m_c Q = \alpha_k (T - T_0) + E\sigma_0 (T^4 - T_{sl}^4) \tag{10}$$

Here Q is the total heat release per a mass unit (fuel calorific value); m_c is the fuel consumption rate (mass flux or combustion rate); α_k is the convective heat transfer coefficient (from the particle to air); E is the emissivity coefficient for a burning particle (or slag); σ_0 is the Stephan-Boltzman constant. Temperatures T, T_0, T_{sl} correspond to experimental values of the temperature of the particle, ambient media, and slag particle.

The procedure of temperature and radiation intensity measurements is as follows. First, the laser beam shutter is closed. The fuel drop is put to the thermocouple edge. The drop diameter is measured by a microscope. The drop is heated from the moment when the PC gives a signal to open the beam shutter. The laser beam heats the drop up to the temperature determined by the experimental conditions.

Figure 5 presents the scheme for combustion of a single fuel drop in different media with various aerodynamic and temperature conditions. The drop may be streamlined by hot gas or vapor, *etc.*

In our experiments on gasification the volatile components together with overheated water vapor were sucked into the primary converter (a gas analyzer developed by the Institute of Thermophysics), then it passes the mechanical filter and the vapor absorber (a filter with silicagel). The water vapor begins to blow the drop only after the moment of shutter opening. The vapor stream was uniform over its cross-section, the mean velocity was W=0.1 m/s, and Reynolds number Re~5.

The data processing was carried out through the scheme: a signal from primary transformers (thermocouple-photodiode-gas analyzer) → amplifier → ACD → computer → printer. All data were read with a frequency of 25 Hz from the computer and treated by the software with outlay to the display and printer.

Measurement results

In our experiments on fuel combustion in air at the standard pressure we measured the drop's temperature and the emission intensity from it. As for water-vapor-gasification, the outlet was obtained from CO and CO_2 measuring by a gas analyzer. The result of this study was the influence of drop's size, content and temperature on dynamics of combustion and gasification. The existence time of a fuel drop, gasification time, ignition temperature, and combustion rate were determined. We also cleared out the relative role of every combustion phase (heating, water evaporation from the coal-water mixture, combustion of volatile components and of coke residue).

Figure 7 presents the dynamics of combustion of a single CWM drop with measuring of the thermometric and color temperatures. The thermocouple (T_t) and

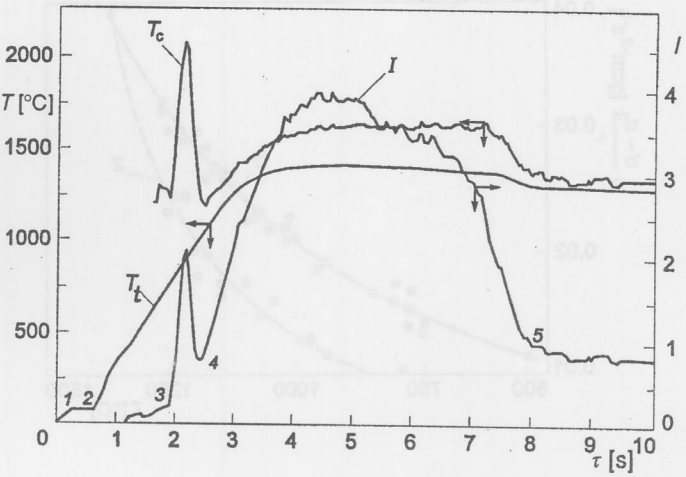

Figure 7. Combustion dynamics for a CWM drop (d = 1.5 mm) from measurements of the thermometric (T_t) and color temperatures (T_c).
0–1 drop heating,
1–2 water evaporation,
2–3 volatile extraction,
3–4 volatile combustion,
4–5 combustion of the coke remaining

photometric (I) measurement lines are supplementary. The initial stages (drop heating and water evaporation) cannot be detected by the photodiode. It measures the particle's radiation intensity at high temperatures (combustion of volatile components and coke). The thermocouple track down the temperature within the particle, but the photo sensor operates from the moment of flaming of volatile components.

The zone *4* in Fig. 7 is characterized by nonstationary discharge of volatile components, by fuel mass decrease and by repulsion of the oxidizer from the combustion surface. This causes a decrease in emission at the stage before the coke burning, which is related with depletion of volatile components. Due to water evaporation and release of volatile components from the drop, the rest of particle conglomerate gain a high-developed inner surface. This big surface facilitates the fuel oxidation resulting in temperature growth and increase in emission, which is detected by the photo sensor.

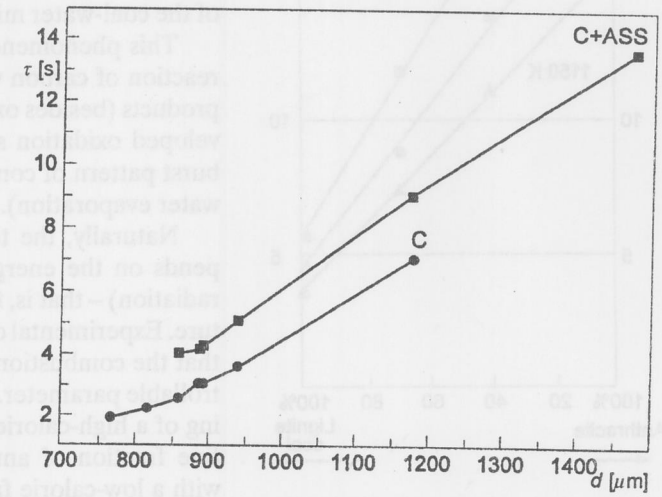

Figure 8. CWM drop combustion time as a function of atomization diameter. *C+ASS – CWM prepared from D–grade coal +5% of ASS–grade coal; C – C+ASS–CWM prepared from D–grade coal*

This experimental technique was applied to

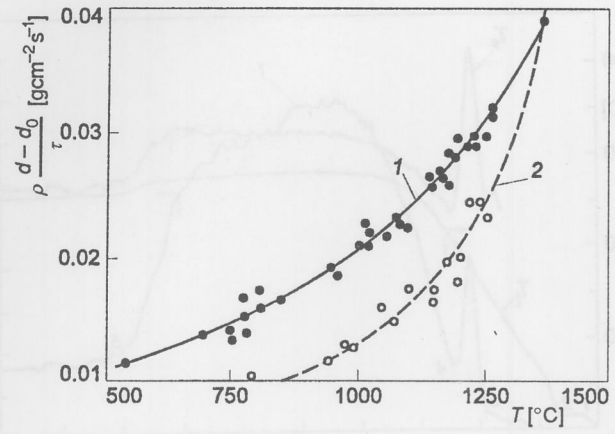

Figure 9. Generalization of experimental data on CWM drop combustion vs. equilibrium combustion temperature.
1 – CWM without drying; 2 – CWM after drying (by laser beam)

drops of different diameters (d = 400–2000 μm) and temperatures in the range of T = 600–1400 °C (Fig. 8). Experimental data were plotted in coordinates $\rho(d - d_0)/\tau$ = f(t) (Fig. 9). Here d_0 is the thermocouple's junction diameter, ρ is the CWM density, and τ is the drop existence time until complete burnout of the coke residue. This time is determined by a sharp drop of the photometric curve to the initial level. This moment almost coincides with stabilization of the temperature-time curve (coke has burnt out). The value $\rho(d - d_0)/\tau$ can be considered as the effective mass rate of fuel drop combustion. One can see that at the same temperature, the combustion mass rate is higher for the drop than for a dry-out particle of the coal-water mixture.

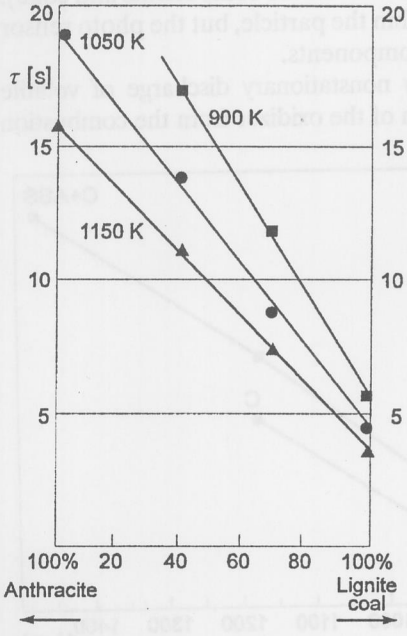

Figure 10. CWM drop's combustion time (d=1.5 mm) measured from the ignition moment, as a function of ASS–coal percentage, lignite and temperature

This phenomenon can be connected with reaction of carbon with vapor decomposition products (besides oxygen), and with highly developed oxidation surface because of microburst pattern of combustion (due to intensive water evaporation).

Naturally, the total combustion time depends on the energy flux to the drop (laser radiation) – that is, from the furnace temperature. Experimental data in Fig. 10 demonstrate that the combustion time for CWMs is a controllable parameter. It can be changed by mixing of a high-calorie low-reactive coal (*e. g.*, a fine fraction of anthracite with grade ASS) with a low-calorie fast-reactive coal (*e. g.*, lignite).

Using the balance equation (10) and experimental data (see Fig. 7), we present in Fig.

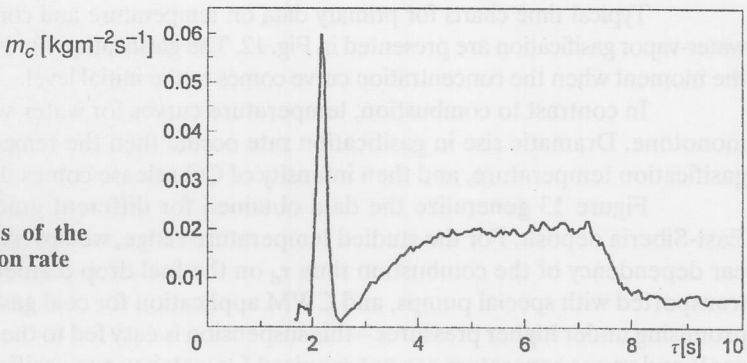

Figure 11. Dynamics of the CWM drop combustion rate

11 the dynamic of fuel drop combustion ($Q \approx 30 \cdot 10^6$ J/kg). A sharp peak in this graph corresponds to the outcome of volatile components with fuel heating. One can see that this time interval is much less than the total time of mass decrease due to combustion.

If we perform experiments on combustion of a small drop in conditions of natural convection, we have the following criteria: $\mathrm{Re} \to 0$, $\mathrm{Gr} = (g\beta\Delta t d^3)/(\nu^2) \approx 40$, and $\mathrm{Nu} = (\alpha_k d/2\lambda) \approx 2.5$ [4].

Our estimates of contribution from the convective and mass terms reveal that they make up about 15% from the radiative heat transfer.

For a carbon particle combustion in air, the Stephan's flux for oxygen diffusion and corresponding reaction products is negligible [7]. Therefore we don't account it in the heat balance.

In some sorts of coal the content of volatile components may be as high as 40%. Their heat-caused emanation takes away some heat from the particle. Unfortunately, the physical properties of multicomponent volatile substance are usually unknown. So we can only estimate this heat loss. However, experimental curves (Figs. 7 and 11) demonstrate that the durability of combustion of volatile components is only a small percentage of the total combustion time.

The mass of burnout coal during the volatile components discharge and their combustion can be calculated from the known percentage of them in the coal and the combustion time chart.

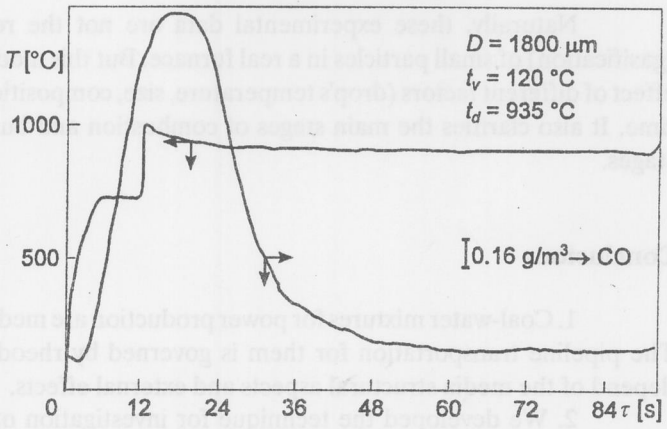

Figure 12. Temperature and concentration evolution for CWM gasification (*D*–grade coal from Kuznetsk); t_v – vapor temperature; t_d – gasification temperature

Typical time charts for primary data on temperature and concentration of CO for water-vapor gasification are presented in Fig. 12. The gasification time was determined from the moment when the concentration curve comes to the initial level.

In contrast to combustion, temperature curves for water-vapor gasification are monotone. Dramatic rise in gasification rate occurs then the temperature achieves the gasification temperature, and then intensity of CO release comes down.

Figure 13 generalize the data obtained for different grades of coal from the East-Siberia deposit. For the studied temperature range, we observed a slightly non-linear dependency of the combustion time τ_d on the fuel drop diameter. Usually CWM is transported with special pumps, and CWM application for coal gasification seems to be promising under higher pressures – this suspension is easy fed to the chamber (unlike dry coal) and vapor generators are not required for water-vapor-gasification.

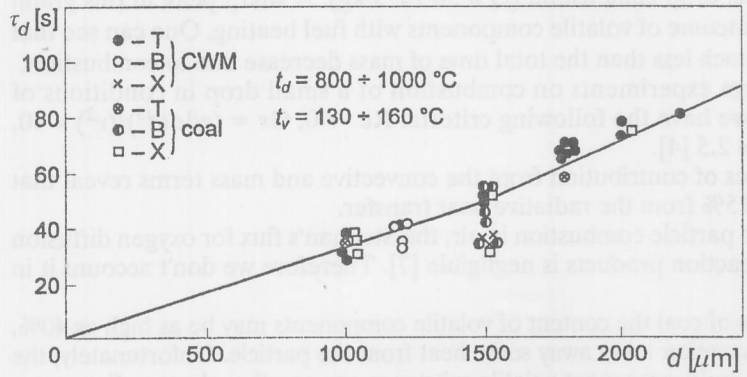

Figure 13. Gasification time for coal particles and CWM drops made of different lignite vs. diameter; t_v – vapor temperature; t_d – gasification temperature; *X*, *T*, *B* – first letter of coal name (see Table 1)

Naturally, these experimental data are not the real pattern of combustion (gasification) of small particles in a real furnace. But this model allows us to estimate the effect of different factors (drop's temperature, size, composition) on the total combustion time. It also clarifies the main stages of combustion and burn-out velocity at different stages.

Conclusions

1. Coal-water mixtures for power production are media with rheology properties. The pipeline transportation for them is governed by rheodynamic parameters, which depend of the media structural aspects and external effects.

2. We developed the technique for investigation of temperature kinetics and concentration during combustion (or gasification) of a single fuel drop. It is based on simultaneous measuring of the thermometric and color temperatures with analysis of the gaseous products composition. These complex measurements give us the total combus-

tion time, duration of different stages of the process (heating, evaporation, combustion of volatile components and coke residue), as well as the combustion mass flow rate.

3. The CWM combustion time can be controlled through adding of fast-reactive fuel to low-reactive fuel.

4. The CWM drop combustion is a multistage process. The specific of this process is the water evaporation from the drop. This makes a high porosity of the particle and enhances the intensity of diffusion combustion.

References

[1] Edward, T. M., Coal-Water Fuel Combustion, 21st Symposium (International) on Combustion, Combustion Institute, 159, 1986

[2] Belkin, I. M., Vinogradov, G. V., Leonov, A. I., Rotation Devices. Measurement of Viscosity and Physical-Chemical Characteristics of Materials (in Russian), Moscow, *Mashinostroenie*, 1968

[3] Khzmalyan, V. M., Kogan, A. Ya., Theory of Combustion and Furnaces (in Russian), Moscow, Energy, 1997

[4] Kantorovich, V. V., Solid Fuel Combustion and Gasification – Foundations of Theory (in Russian), Moscow, Izd. AN SSSR, 1958

[5] Burdukov, A. P., Karpenko, E. I. *et al.*, Experimental Study of the Combustion Dynamics of Coal-Water Suspension Drops, *Combustion, Explosion and Shock Waves, 32* (1996), 4, pp. 412–415

[6] Gordov, A. N., Foundations of Pyrometry, Metallurgia, (1971), p. 158

[7] Foundations of the Combustion Theory (Ed. by V.V. Pomerantsev), Moscow, *Energoatomizdat*, 1986, p. 310

Authors' address:

A. P. Burdukov, V. P. Popov, V. D. Fedosenko
The Institute of Thermophysics,
Siberian Branch, Russian Academy of Science
Novosibirsk, Russia

Paper submited: April 23, 1999
Paper revised: October 4, 1999
Paper acepted: November 3, 1999